

# The Initial Array Configuration for ASKAP

Neeraj Gupta, Simon Johnston, Ilana Feain & Tim Cornwell  
Australia Telescope National Facility, CSIRO

October 13, 2008

## Executive Summary

The science case for ASKAP (Johnston et al. 2007) was written without specific configuration details. Subsequently, science priorities for ATNF telescopes in general and ASKAP in particular were presented in *ATNF Science in 2010-2015* by Ball et al. (2008) and this priority listing strongly influenced the configuration decision. Input from the community at large and the ASKAP Science Working Group were also taken into consideration. An initial discussion paper for ASKAP configurations was given by Feain et al. (2008) with the technical studies presented in Gupta et al. (2008). We recommended that the best initial option for the configuration was a hybrid array optimised for the HI emission surveys.

The overall ASKAP budget envelope has since established that the initial configuration will consist of 36 antennas. The configuration derived in this paper has 30 of the antennas arranged within a circle of diameter  $\sim 2$  km, with a further 6 antennas arranged to form a Reuleaux triangle with maximum separation of  $\sim 6$  km. The configuration takes into account a mask of the site at the Murchison Radio Observatory.

The initial ASKAP configuration is optimised to produce excellent sensitivity and a good point spread function (sidelobe levels 2-3%) at an angular resolution of  $30''$  at 1.4 GHz. The configuration also provides high survey speed at an angular resolution of  $10''$  and good surface brightness sensitivity at angular resolutions of  $60''$  and  $90''$ . We expect that this configuration will return excellent science outcomes for ASKAP for at least the first five years of its operation.

# 1 Introduction

ASKAP is a next generation radio telescope on the strategic pathway towards the staged development of the SKA. ASKAP has four goals:

1. to demonstrate and prototype the technologies for the mid-frequency SKA, including field-of-view enhancement by focal-plane phased arrays on new-technology 12-metre class parabolic reflectors,
2. to carry out world-class, groundbreaking observations directly relevant to the SKA Key Science Projects,
3. to establish a site for radio astronomy in Western Australia where observations can be carried out free from the harmful effects of radio interference.
4. to establish a user community for SKA.

ASKAP will become operational from 2012, SKA Phase I will become operational from  $\sim$ 2015 and full SKA will become operational from  $\sim$ 2020. The *default* lifetime of ASKAP is 30 years and current planning assumes this default. However, the *practical* lifetime of ASKAP is likely to be much shorter if the Murchison Radio Observatory is chosen as the site for the SKA — this decision will be made in 2011–12. Regardless of where the SKA is built, it is crucial that ASKAP return the best science outcomes during its first 5-7 years of operation; this is ASKAP's *competitive* lifetime. Beyond this time, ASKAP will be superseded by SKA phase I, and eventually SKA.

A summary of the science case for ASKAP was presented in Johnston et al. (2007) with a more complete version in Johnston et al. (2008). The science case was written before the exact number of antennas was known and without a specific configuration; the only constraint was that the maximum baselines be less than  $\sim$  8 km. The science priorities for ASKAP in the period 2010-2015 are presented as part of the Ball et al. (2008) document *ATNF Science Priorities in 2010-2015*. As listed in that document, the order of science priorities for ASKAP is:

- Understanding galaxy formation and gas evolution in the nearby Universe through extragalactic HI surveys, including near-field cosmology
- The characterisation of the radio transient sky through detection and monitoring (including VLBI) of transient and variable sources
- Determining the evolution, formation and population of galaxies across cosmic time via high resolution, confusion-limited, continuum surveys
- Exploring the evolution of magnetic fields in galaxies over cosmic time through polarisation surveys

Since the time of writing of those documents, the number of antennas available to ASKAP has been finalised to be 36. In this document we present the initial ASKAP configuration, show the UV coverage and beam shapes for various declinations and describe the sensitivity as a function of angular resolution.

## 2 Configuration

The science priorities, in conjunction with the recommendations in Feain et al. (2008), the studies by Gupta et al. (2008) and community consultation have resulted in the initial configuration of ASKAP which seeks to maximise the sensitivity for extragalactic HI surveys (Staveley-Smith 2006, 2008) whilst also providing high resolution and good surface brightness sensitivities.

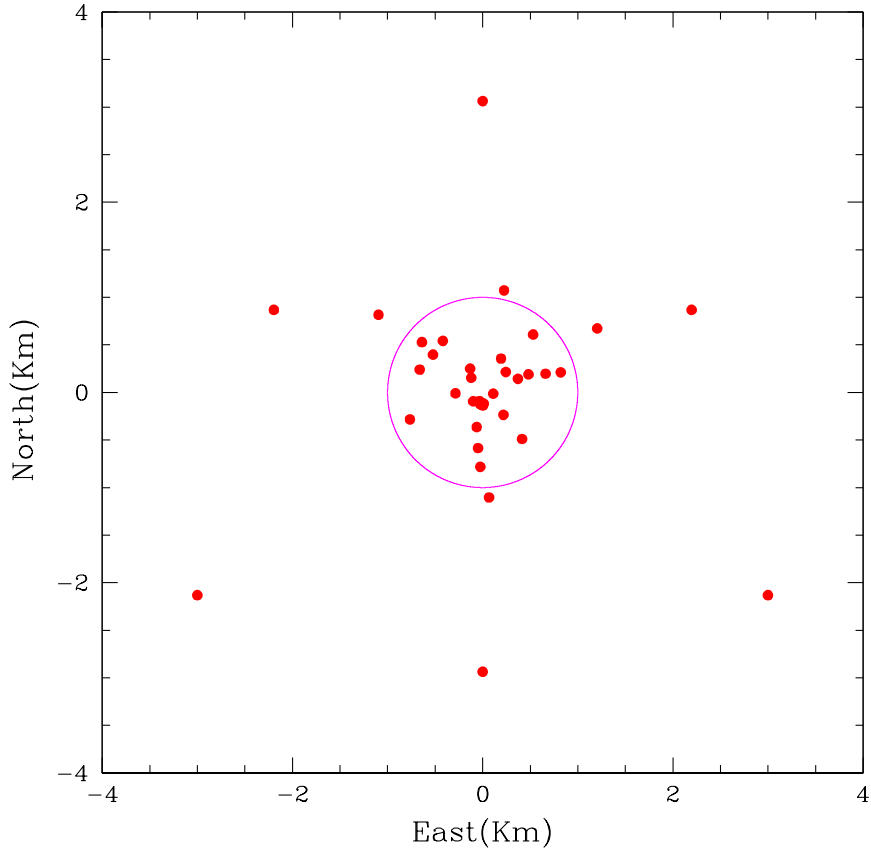


Figure 1: Layout of the 36 antennas of the initial ASKAP configuration. The circle has a radius of 1 km.

To achieve this, the locations of 27 antennas were optimised using AntConfig (de Villiers 2007) to produce a Gaussian distribution of visibilities with a scale of  $\sim 700$  m, corresponding to a point spread function of  $\sim 30''$ . Three antennas were then added to the core of the configuration to provide short spacings ( $\sim 20 - 100$  m) to enhance the low surface brightness sensitivity. Finally, six antennas were arranged to form a Reuleaux triangle with a maximum separation of  $\sim 6$  km. The layout of the 36 antennas is shown in Figure 1. The configuration has a smallest antenna separation of 22 m, and a longest separation of 6 km. ASKAP is located on the Murchison Radio Observatory in the Murchison Shire of Western Australia. The longitude and latitude, corresponding to the 0,0 coordinate in Figure 1 are approximately 116.5 east and 26.7 south.

### 3 UV coverage and beams

There are 630 baselines in the 36 antenna configuration for ASKAP. For illustrative purposes we show the UV coverage for a 10 hr track of a source at  $-50$ ,  $-30$ ,  $-10$ ,  $0$  and  $+10$  declination in Figure 2 and the snapshot (12 min) coverage for the same declinations in Figure 3. The frequency of the observation is 1.4 GHz and a narrow band (0.02 MHz) has been assumed (no multi-frequency synthesis). In Table 1 we summarise the size of the naturally weighted synthesised beam for different declinations and integration times. An elevation limit of  $15^\circ$  was assumed for the antennas. Good circularity of the beam is maintained through a large declination range including declination  $0$  where currently much optical survey data is taken. The sidelobe levels of the beams are 3-4% over the entire declination range given in Table 1 except for  $\pm 3^\circ$  centered at declination  $0^\circ$ . In this range the sidelobe levels get worse by a factor 2-3.

Table 1: Full width half maximum of the point spread function (beam size) as a function of declination for the initial ASKAP configuration for integration times of 12 min and 10 hr. Natural weighting of the visibilities is assumed.

Declination (deg)	Snapshot beam (arcsec x arcsec)	10 hr beam (arcsec x arcsec)
$-50$	19.1 x 15.4	19.4 x 15.9
$-30$	17.6 x 15.2	18.9 x 17.5
$-10$	17.9 x 15.3	19.6 x 18.2
$0$	18.4 x 15.3	19.5 x 19.3
$+10$	21.5 x 15.1	20.1 x 19.2

### 4 Configuration Sensitivity

The sensitivity of the configuration at various angular scales is an important metric for ASKAP. The configuration is designed to optimise sensitivity on angular scales of  $30''$  (for HI emission surveys; see Staveley-Smith 2006, 2008), whilst also providing good low surface brightness sensitivity (at low angular resolution) and high resolution imaging capability (see Condon 2007).

Sensitivity as a function of angular resolution is given in Figure 4, presented in two panels for clarity. The naturally weighted beam gives maximum sensitivity and an angular resolution of just under  $20''$  (see Table 1). This is indicated by the black square in Figure 4. Gaussian tapering was applied to the data with progressively larger and larger values, resulting in the curve shown in the left hand panel of Figure 4. In order to get higher resolution than that available with natural weighting it is necessary to downweight the short baselines at the expense of the longer baselines. This can be achieved through robust weighting (Briggs 2002) and the results are shown on the right hand panel of Figure 4.

Survey speeds and sensitivity for an interferometer like ASKAP have been derived elsewhere (e.g. Johnston & Gray 2006). To summarise, the time,  $t$ , required to reach a given

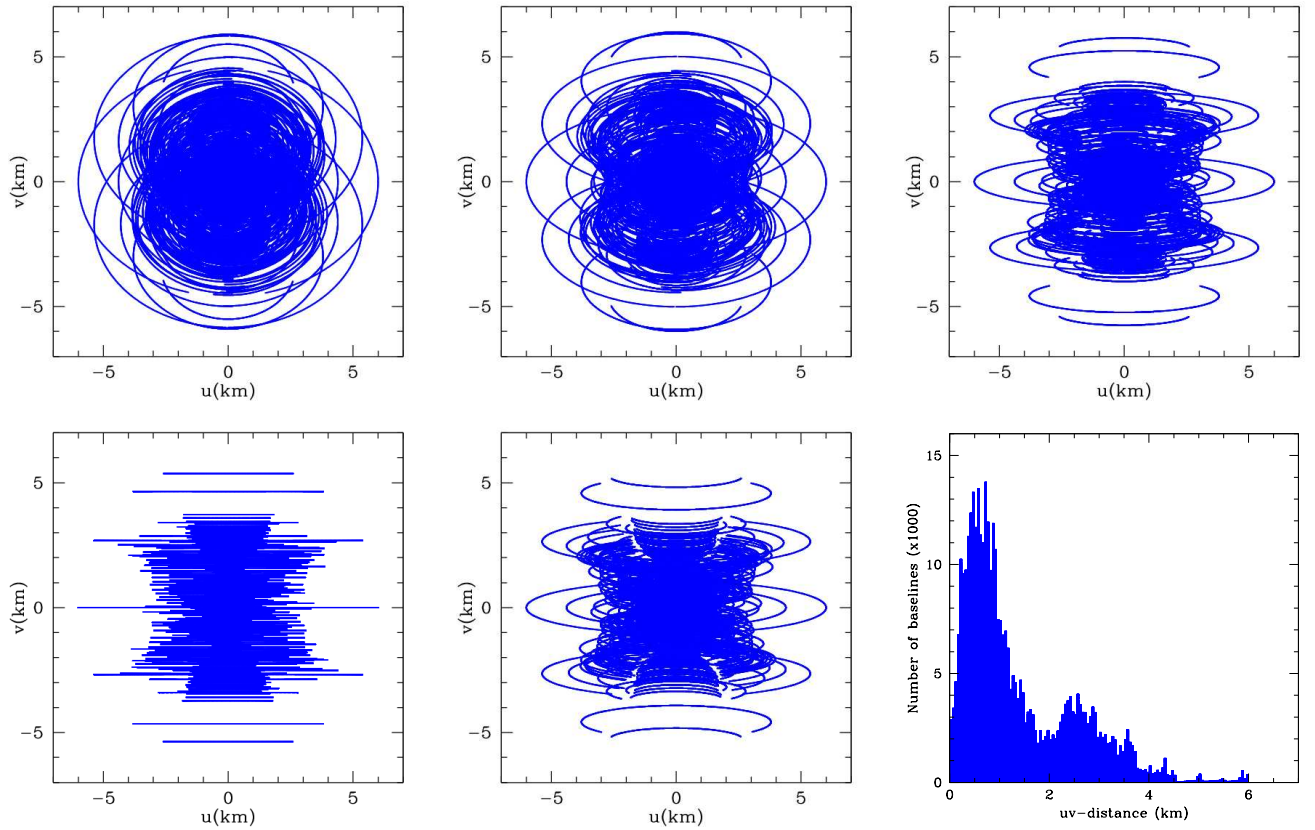


Figure 2: UV coverage for a 10 hr track of a source at (from left to right and top to bottom)  $-50$ ,  $-30$ ,  $-10$ ,  $0$ ,  $+10$  declination at an observing frequency of 1.4 GHz. The final panel shows the baseline distribution for the  $-50$  declination case.

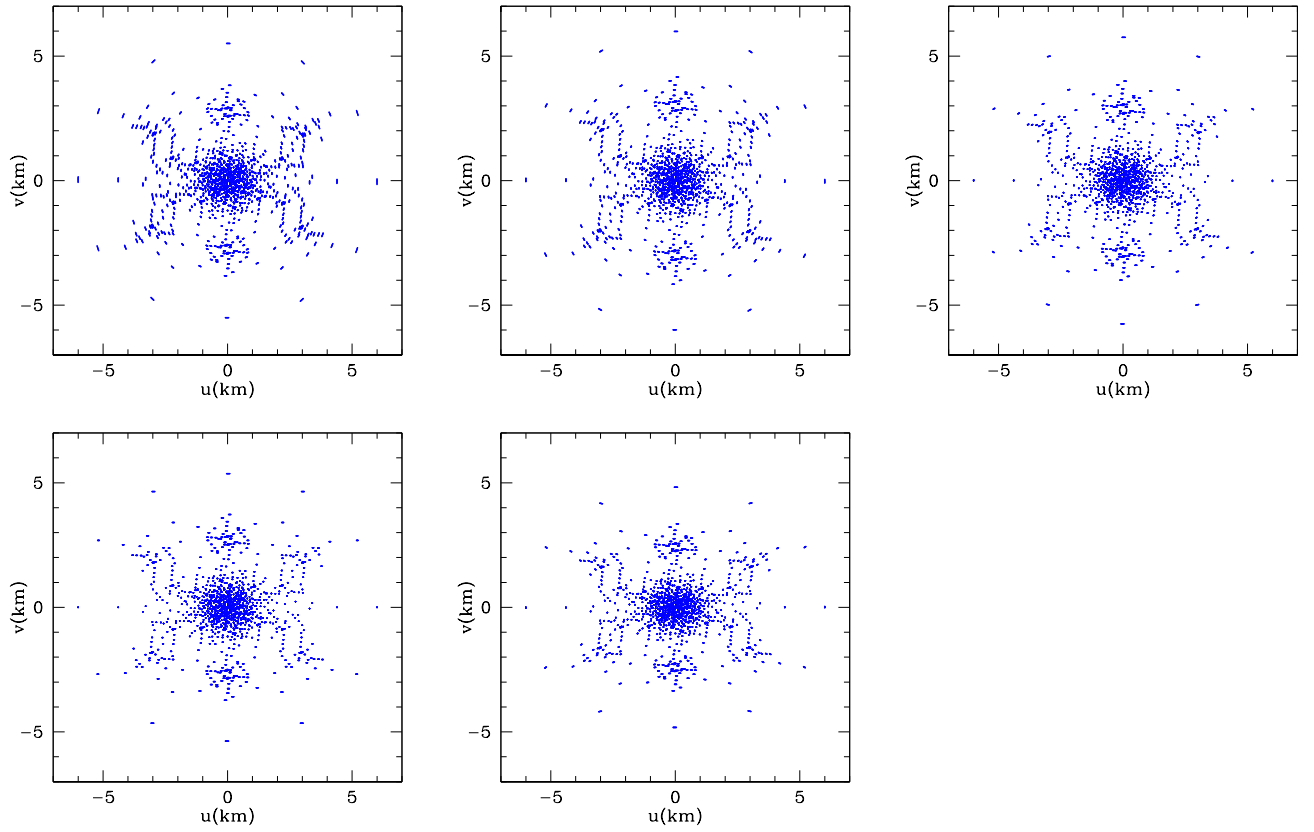


Figure 3: Snapshot (12 min) UV coverage of a source at (from left to right and top to bottom)  $-50$ ,  $-30$ ,  $-10$ ,  $0$ ,  $+10$  declination at an observing frequency of 1.4 GHz.

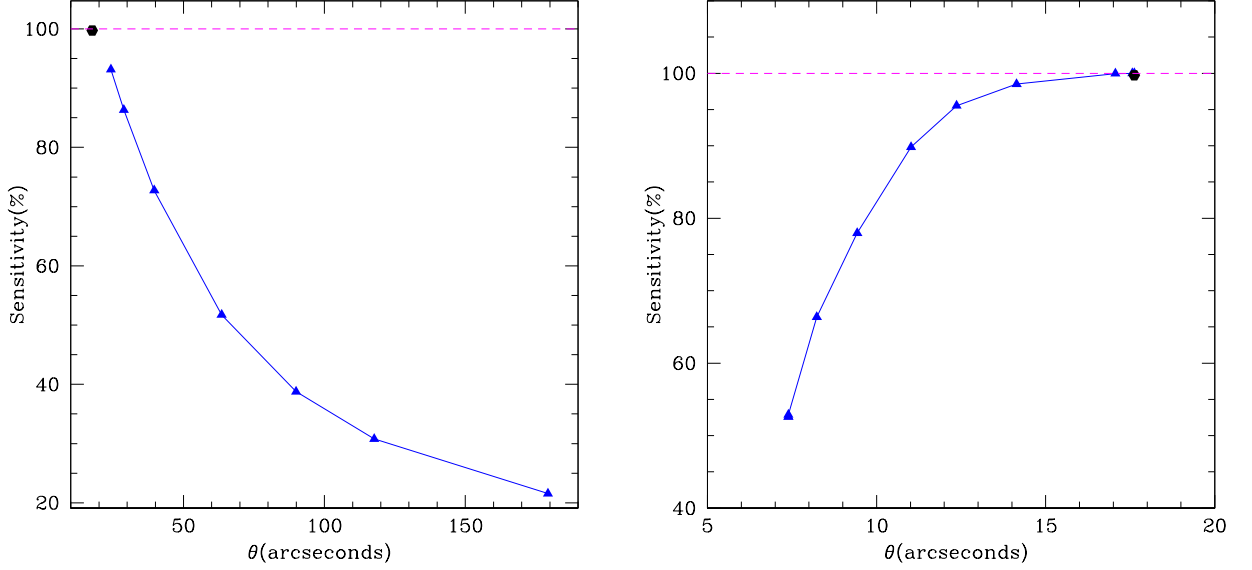


Figure 4: Sensitivity as a function of the full width half maximum of the point spread function for the ASKAP configuration. Left panel: Gaussian tapering of the data was applied and the results compared with the sensitivity obtained through natural weighting (solid black point). Right panel: Robust weighting was applied and the results compared with the sensitivity obtained through natural weighting (solid black point).

sensitivity limit for point sources,  $\sigma_s$ , is

$$t = \left( \frac{2 k T}{A N \epsilon_a \epsilon_c} \right)^2 \frac{1}{\sigma_s^2 B n_p} \quad (1)$$

where  $B$  is the bandwidth (Hz),  $n_p$  the number of polarizations,  $A$  is the collecting area of a single element ( $\text{m}^2$ ),  $N$  is the number of elements and  $\epsilon_a$  and  $\epsilon_c$  represent dish and correlator efficiencies. The system temperature is  $T$  with  $k$  being the Boltzmann constant. The number of square degrees per second that can be surveyed to this sensitivity limit is

$$SS_s = F B n_p \left( \frac{A N \epsilon_a \epsilon_c \sigma_s}{2 k T} \right)^2 \quad (2)$$

where  $F$  is the field of view in square degrees. The surface brightness temperature survey speed is given by

$$SS_t = F B n_p \left( \frac{\epsilon_c \sigma_t}{T} \right)^2 f^2 \epsilon_s^{-2} \quad (3)$$

where now  $\sigma_t$  denotes the sensitivity limit in K and  $f$  relates to the filling factor of the array via

$$f = \frac{A \epsilon_a N \Omega \epsilon_s}{\lambda^2} \quad (4)$$

Here,  $\epsilon_s$  is a ‘synthesised aperture efficiency’ which is related to the weighting of the visibilities and is always  $\leq 1$ .

In Table 2 we list values of the survey speed for different ‘typical’ surveys for different angular resolutions. The first entry gives a continuum survey where the entire 300 MHz of

Table 2: Survey speeds for different angular resolutions under the assumption of a 50 K system temperature and an aperture efficiency of 0.8.

Parameter	10''	18''	30''	90''	180''	
Continuum survey speed (300 MHz, 100 $\mu$ Jy)	220	361	267	54	17	deg <sup>2</sup> /hr
Line survey speed (100 kHz, 5 mJy)	184	301	223	45	14	deg <sup>2</sup> /hr
Surface brightness survey speed (5 kHz, 1 K)	-	-	1.1	18	94	deg <sup>2</sup> /hr

Table 3: Sensitivity for a one hour observation at different angular resolutions under the assumption of a 50 K system temperature and an aperture efficiency of 0.8.

Parameter	10''	18''	30''	90''	180''	
Continuum sensitivity (300 MHz)	37	29	34	74	132	$\mu$ Jy/bm
Line sensitivity (100 kHz)	2.1	1.6	1.9	4.1	7.3	mJy/bm
Surface brightness sensitivity (5 kHz)	-	-	5.2	1.3	0.56	K

bandwidth is exploited and a desired sensitivity of 100  $\mu$ Jy is required. The second entry gives a spectral line survey, with the third line listing a surface brightness survey needing to reach 1 K rms over 5 kHz channel. Table 3 lists the sensitivity after 1 hr of observation for the different surveys.

## 5 Notes

A full site survey has not yet been carried out at time of writing (October 2008). Results from the site survey may alter the position of some of the antennas in this layout. The system temperature and aperture efficiency are still not well determined but should become better known towards the middle of 2009.

## Acknowledgments

We thank Robert Braun, Jim Condon and Lister Staveley-Smith for useful discussions and contributions. We acknowledge the use of casapy for our simulations.

## References

- Ball, L., 2008, ATNF Science in 2010–2015.  
 Briggs, D., 2002, PhD Thesis  
 Condon, J., 2008, ATNF SKA Memo Series, 015  
 de Villiers M., 2007, A&A, 469, 793  
 Feain, I., Johnston, S., Gupta, N., ATNF SKA Memo Series, 017  
 Gupta, N., Johnston, S., Feain, I., ATNF SKA Memo Series, 016  
 Johnston S. et al., 2007, PASA, 24, 174

Johnston et al. 2008, Experimental Astronomy, In Press  
 Staveley-Smith L., 2006, ATNF SKA Memo Series, 006  
 Staveley-Smith L., 2008, ATNF SKA Memo Series, 020

For the ATNF SKA Memo Series see the web pages at  
<http://www.atnf.csiro.au/projects/askap/Memoseries.html>

## Appendix A

Table 4: Antenna locations for the layout shown in Figure 1

No.	x-location (m)	y-location (m)	No.	x-location (m)	y-location (m)
1	-175.23	-1673.46	2	261.11	-796.92
3	-29.20	-744.43	4	-289.35	-586.93
5	-157.03	-815.57	6	-521.31	-754.67
7	-1061.11	-840.54	8	-921.82	-997.62
9	-818.29	-1142.27	10	-531.75	-850.72
11	81.35	-790.24	12	131.12	-1208.83
13	-1164.70	-316.77	14	-686.24	-590.28
15	-498.98	-506.33	16	-182.24	-365.11
17	420.84	-811.08	18	804.10	-1273.32
19	-462.81	-236.35	20	-449.77	-15.03
21	13.79	-110.97	22	-425.68	181.90
23	-333.40	503.60	24	-1495.47	-1416.06
25	-1038.57	-1128.36	26	-207.15	-956.31
27	-389.05	-482.40	28	-434.00	-510.00
29	-398.00	-462.00	30	-425.00	-475.00
31	-400.00	-3664.00	32	1796.00	-1468.00
33	2600.00	1532.00	34	-400.00	2336.00
35	-3400.00	1532.00	36	-2596.00	-1468.00